arXiv:cond-mat/0203115v1 [cond-mat.mes-hall] 6 Mar 2002

CHESSBOARD MAGNETOCONDUCTANCE OF A QUANTUM DOT IN THE KONDO REGIME

C. TEJEDOR
Departamento de Física Teórica de la Materia Condensada,
Universidad Autónoma de Madrid,
Cantoblanco, 28049, Madrid, Spain.

AND

L. MARTIN-MORENO
Departamento de Física de la Materia Condensada,
Universidad de Zaragoza,
Zaragoza 50015, Spain.

Abstract. Transport through a quantum dot (QD) in the Kondo regime shows alternating regions of high and low conductance when both an external magnetic field and the gate potential controlling the depth of the QD potential are varied. We present a theoretical analysis of this chessboard aspect of the magneto-conductance. An effective Kondo Hamiltonian is obtained by means of a restriction to the Hilbert space supported by just a few low energy states of N and $N \pm 1$ electrons in the QD. We obtain antiferromagnetic exchange couplings depending on tunneling amplitudes and correlation effects. When either the magnetic field or the number of electrons in the QD is varied, Kondo temperature shows large oscillations due to the successive appearance of ground states having strong and weak correlation effects alternatively.

1. Introduction

Many theoretical predictions[1, 2, 3, 4, 5, 6, 7] on the Kondo physics in a quantum dot (QD) have been experimentally observed[8, 9, 10, 11, 12, 13]. However, the use of a standard Anderson Hamiltonian does not allow a complete understanding of some other experiments as those devoted to measure the phase-shift of electrons passing through the QD[14, 15] or those

presenting a chessboard aspect of the QD conductance in the quantum Hall regime[16, 17, 18]. Correlation effects within the QD[19, 20] are probably essential for the understanding of the experimental results.

This paper is devoted to the theoretical analysis of the experimental Kondo-like conductance of a QD in the quantum Hall regime. For a given number N of electrons in the QD, the system presents alternating high and low conductance regions as a function of an external magnetic field B. When N is varied in ± 1, the high and low conductance valleys are interchanged. Therefore, the representation of the conductance (in a grey scale) as a function of both B and a gate potential which allows to vary N, takes the aspect of a chessboard[16, 17, 18]. An interesting piece of experimental information on the density of states is obtained from the differential conductance measured when a source-drain bias is applied. In such experiment[16, 17], one observes a double peak with a separation which remains practically constant when the magnetic field is varied. This suggests that two (split) states are playing an important role in the conduction process.

Our description for the Kondo physics in a QD in the presence of a high magnetic field is valid for any number of electrons (even or odd without restriction to 1 or 2) and any value of the QD spin S_z (not restricted to 0, 1 for even N or 1/2 for odd N). Instead of describing spin-flip scattering in terms of spin-ladder operators $S^{(\pm)}$, we find a set of spin-flip Hubbard operators describing a collective spin effect of all the N electrons contained in the QD. Despite both N and S_z can be very large, the scattering of carriers only produces transitions between two many-body states of the QD with S_z differing in ± 1. These many-body states are of two types: some of them are "practically" just one Slater determinant, i.e. not presenting correlation effects, while some others are a linear combination of many configurations, i.e. involving strong correlation effects. This is going to produce strong oscillations in the Kondo temperature. We find this is the physical reason of the appearance of the chessboard aspect of the conductance instead of the other obvious possibility of having alternating ferro and antiferro exchange couplings. In fact, we find that the spin-flip process can be described by a Kondo Hamiltonian with antiferromagnetic couplings which depend on both tunneling amplitudes and correlation effects.

The steps of our description are the following:

1. Hamiltonian for N interacting electrons in a QD coupled to two leads.
2. Numerical calculation of the spectrum of N electrons in the isolated QD which involves three energy scales: confinement, Zeeman and interaction.
3. Two alternating types of ground states (GS): strong correlation and weak correlation.

4. Projection onto the subspace of the (two) lowest eigenstates and coupling to the leads.
5. An effective Kondo Hamiltonian with antiferromagnetic exchange couplings depending on the QD properties (Spectral amplitudes) is obtained.
6. Strong oscillations of the Kondo temperature due to strong oscillations of the spectral amplitude for strongly and weakly correlated states.
7. Experiment at finite temperature $\Rightarrow$ oscillations (Chessboard aspect) of the conductance.

2. QD spectrum (Steps 1 to 3)

We consider N electrons in the presence of a magnetic field and confined in a QD coupled to leads. The Hamiltonian is

$$H = H_{QD} + H_L + H_{TUN}. \tag{1}$$

The first term in Eq. (1) describes an isolated QD. For a parabolic QD in the presence of a magnetic field and including interaction between the electrons, the QD Hamiltonian is described by (hereafter we take $\hbar = 1$)

$$H_{QD} = \sum_i \varepsilon_{i,\sigma} d^\dagger_{i,\sigma} d_{i,\sigma} + g\mu_B B S_z + \frac{1}{2} \sum_{i_j,\sigma_j} V_{i_1 i_2 i_3 i_4} d^\dagger_{i_1,\sigma_1} d^\dagger_{i_2,\sigma_2} d_{i_3,\sigma_3} d_{i_4,\sigma_4}. \tag{2}$$

The first term in (2) involves the energy scale related with potential and magnetic confinement. $i = \{n, m\}$ is an index containing both the Landau level index n and the third component of the angular momentum m.

$$\varepsilon_{i,\sigma} = \left[\frac{1}{2} + \frac{1+\gamma}{2} n + \frac{1-\gamma}{2} m\right] \Omega \tag{3}$$

is the single particle eigenvalue depending on both the QD confinement ω_0 and cyclotron ω_c frequencies through $\Omega = \sqrt{\omega_c^2 + 4\omega_0^2}$ and $\gamma = \omega_c/\Omega$. $d^\dagger_{i,\sigma}$ creates an electron with Landau index n, angular momentum m and spin σ in the QD. The second term in Eq. (2) introduces the Zeeman energy scale with g being the Landé g-factor. The interaction energy scale appears in the last term, electron-electron repulsion. The Coulomb interaction matrix elements $V_{i_1 i_2 i_3 i_4}$ have a typical energy scale $e^2/\varepsilon l_B$, where ε is the dielectric constant and $l_B = 1/\sqrt{m\Omega}$ the magnetic length.

The second term in Eq. (1)

$$H_L = \sum_{k,\sigma} \varepsilon_{k,\sigma} c^\dagger_{k,\sigma} c_{k,\sigma} \tag{4}$$

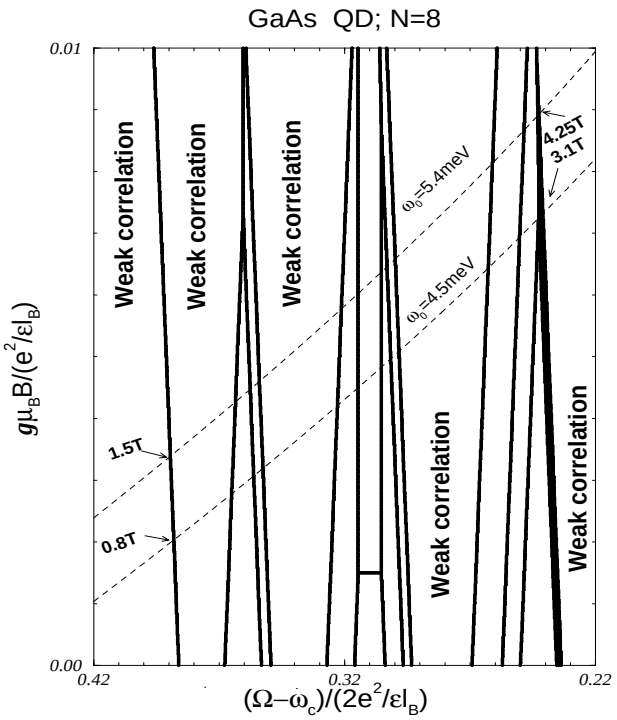

Figure 1. Phase diagram of the possible GS of a GaAs QD with 8 electrons at $2 > \nu > 1$. The axes contain kinetic $(\Omega - \omega_c)/(2e^2/\varepsilon l_B)$ and Zeeman $g\mu_B B/(e^2/\varepsilon l_B)$ contributions to the energy. The regions labelled as *weak correlation* correspond to compact states from $|C_4^4\rangle$ ($\nu = 2$) at the left to $|C_8^0\rangle$ ($\nu = 1$) at the right. The unlabelled regions correspond to GS showing strong correlation effects (skyrmion-like states, see text). Dashed lines depict, for two different values of the QD confinement frequency ω_0, the evolution of the GS within the range of magnetic fields given at the edges of the lines.

describes, in a single-particle approach, the leads having electrons with quantum numbers k, σ occupying states up to the Fermi energy ε_F.

Finally the tunneling part of the Hamiltonian (1)

$$H_{TUN} = \sum_{k,i,\sigma} V_i \left(d^\dagger_{i,\sigma} c_{k,\sigma} + c^\dagger_{k,\sigma} d_{i,\sigma} \right) \tag{5}$$

is written without any dependence on k of the tunneling amplitudes V_i (taken as real positive) but retain the dependence on i because is going to produce physical consequences.

H_{QD} can be numerically diagonalized for a significantly broad range of N and B, as discussed in many theoretical papers[21]. We have performed calculations including $n = 0, 1$ which means we are able to analyze filling

factors ν below 4, i.e. the regime of experimental interest [16, 17]. Fig. 1 shows results for the GS of $N = 8$ for B large enough to have electrons occupying states only with the lowest Landau index $n = 0$, i.e. $\nu \leq 2$. Dashed lines in Fig. 1 depict, for two different values of ω_0, the evolution of the GS for a GaAs QD within the range of magnetic fields (perpendicular to the QD) given at the edges of the lines. The first observation is that there are two type of regions: 5 regions, labelled as weak correlation, correspond to GS which are practically just one single Slater determinant (or configuration). The other regions correspond to GS which are a linear combination of many configurations. In other words, there are regions with GS having weak correlation and regions with GS having strong correlations. This trend also occurs for calculations in other situations of N and B. In the particular case of Fig. 1, GS's in the weak correlation regions are compact states of the form

$$|C^K_{N-K}\rangle = \prod_{m=0}^{K-1} d^\dagger_{n=0,m,\downarrow} \prod_{m=0}^{N-K-1} d^\dagger_{n=0,m,\uparrow}|0\rangle \tag{6}$$

where $|0\rangle$ is the vacuum state. In going from left to right, one finds successively the states $|C^4_4\rangle$ ($\nu = 2$), $|C^3_5\rangle$, $|C^2_6\rangle$, $|C^1_7\rangle$ and $|C^0_8\rangle$ ($\nu = 1$). In the case of Fig. 1, strongly correlated states have a very peculiar shape: they are skyrmion-like states of topological charge 1 [19, 22, 23]. While the occurrence of compact states is general in the calculations we have performed, in many of such calculations we have not been able to identify the particular nature of the highly correlated GS that always exist.

Fig. 2 shows the evolution of the GS properties with increasing B for the system of Fig. 1 for a typical value [24] $\omega_0 = 5.4$meV. The GS energy E_{GS} has a kink any time a crossing of states occurs. The relevant information on these crossings is the energy splitting $\Delta E = E_{exc} - E_{GS}$ between the lowest excited state and the GS as shown in part (a) of the figure. The spin S_z and the third component M of the total angular momentum of the GS are also given in (b) and (c) respectively. The general trend of interest for us is that GS changes many times when B is varied. For many values of the field, the energy difference between the two lowest states is very small. Moreover, in almost all the cases, these two states have spins differing in 1 while they have different M.

3. Kondo Hamiltonian (steps 4 to 5)

As we mentioned in the introduction, experiments [16, 17] show that the density of states presents a double peak very stable with B. As a consequence of both this experimental fact and the above numerical results, we consider that the main physics of the problem is captured by a two level

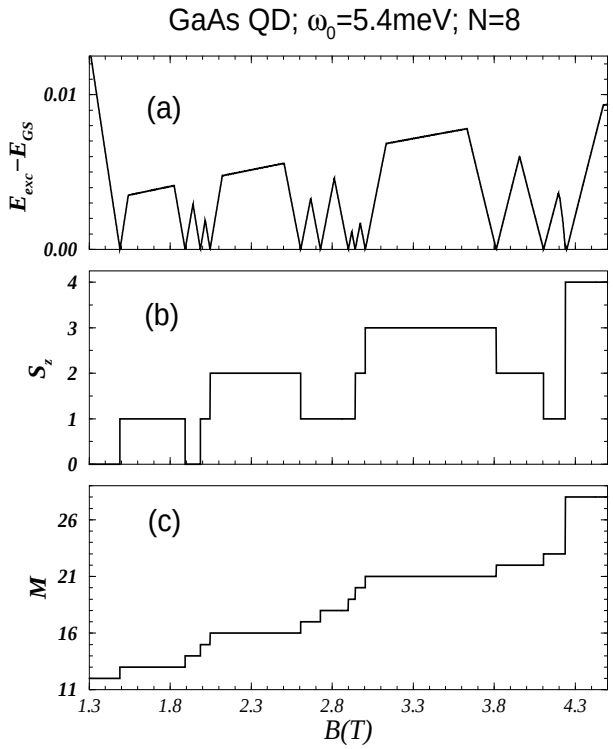

Figure 2. Evolution with the magnetic field B of different magnitudes for the GS of a GaAs QD with $N = 8$ and $\omega_0 = 5.4$meV. Energies are measured in units of $e^2/\varepsilon l_B$. The left side of the figure corresponds to $\nu = 2$ and the right side to $\nu = 1$.

system approach [25]. We project the problem of a N electrons in a QD affected by a high magnetic field onto the subspace subtended by the two lowest energy states $|N, \Uparrow\rangle$ and $|N, \Downarrow\rangle$ with $M_\Uparrow \neq M_\Downarrow$ and spins differing in 1, i.e. $\langle N, \Uparrow |S_z|N, \Uparrow\rangle = \langle N, \Downarrow |S_z|N, \Downarrow\rangle + 1$. H_{TUN} mixes these states with states $|N \pm 1\rangle$ in which $N \pm 1$ electrons are in the QD. In our two level system description, the tunneling Hamiltonian is projected onto the subspaces subtended by the two states for N electrons and the connecting $|N \pm 1\rangle$ electron states. In this process, we consider the connecting $|N \pm 1\rangle$ states as non-degenerate which is the most common case. If either $|N+1\rangle$ or $|N-1\rangle$ is also degenerate, the algebra is more complicated but the physics is the same. Using the notation $\Sigma \equiv \{\Uparrow, \Downarrow\}$, we introduce the tunneling spectral amplitudes

$$\Delta_{-,\Sigma} = \sum_{i,\sigma} V_i \langle N-1|d_{i,\sigma}|N, \Sigma\rangle$$

$$\Delta_{+,\Sigma} = \sum_{i,\sigma} V_i \langle N+1 | d^\dagger_{i,\sigma} | N, \Sigma \rangle \tag{7}$$

and the spin-flip Hubbard operators

$$X_{\Sigma,\Sigma'} = |N,\Sigma\rangle\langle N,\Sigma'|. \tag{8}$$

The projected tunneling Hamiltonian $\overline{H}_{TUN}$ describes the interaction between the QD with N electrons and the leads. An effective coupling is obtained by a standard scattering description [26] including all the possible intermediate states $|I\rangle$ up to second order:

$$\begin{aligned} H_{eff} &= \sum_I \frac{\overline{H}_{TUN}|I\rangle\langle I|\overline{H}_{TUN}}{E^N_{GS} - E_I} \\ &= \sum_{k,k',\Sigma} \Bigg[\frac{\Delta^2_{-,\Sigma}\delta_{k,k'} X_{\Sigma,\Sigma}}{E^N - E^{N-1} - \varepsilon_F} + \frac{\Delta^2_{+,\Sigma} c^\dagger_{k',\sigma} c_{k,\sigma}}{E^N - E^{N+1} + \varepsilon_F} \\ &+ \sum_{\Sigma'} \left(\frac{\Delta_{+,\Sigma}\Delta_{+,\Sigma'}}{E^{N+1} - \varepsilon_F - E^N} + \frac{\Delta_{-,\Sigma}\Delta_{-,\Sigma'}}{E^{N-1} + \varepsilon_F - E^N} \right) X_{\Sigma,\Sigma'} c^\dagger_{k',\sigma'} c_{k,\sigma} \Bigg], \end{aligned} \tag{9}$$

where we have neglected the energy difference between the two states of N electrons. Due to spin conservation, Σ has the same direction than σ and Σ' the same than σ'. The first term is simply a constant. The second term (involving $c^\dagger_{k',\sigma} c_{k,\sigma}$) represents a potential scattering which does not involve any spin flip. These two terms are identical to the ones appearing when building up an *sd* Hamiltonian from the Anderson Hamiltonian in the case of $N = 1$ [26]. As it is usually done in that case, one can forget about these two terms which do not contain anything important for the physics we want to address.

The interesting physics is included in the third term of (9) which is a Kondo Hamiltonian

$$H_K = \sum_{k,k'} \left[J \left(X_{\Uparrow,\Downarrow} c^\dagger_{k'\downarrow} c_{k,\uparrow} + X_{\Downarrow,\Uparrow} c^\dagger_{k',\uparrow} c_{k,\downarrow} \right) + J_\Uparrow X_{\Uparrow,\Uparrow} c^\dagger_{k',\uparrow} c_{k,\uparrow} + J_\Downarrow X_{\Downarrow,\Downarrow} c^\dagger_{k',\downarrow} c_{k,\downarrow} \right], \tag{10}$$

with exchange couplings

$$J = \frac{\Delta_{+,\Uparrow}\Delta_{+,\Downarrow}}{E^{N+1} - \varepsilon_F - E^N} + \frac{\Delta_{-,\Uparrow}\Delta_{-,\Downarrow}}{E^{N-1} + \varepsilon_F - E^N} \tag{11}$$

$$J_\Sigma = \frac{\Delta^2_{+,\Sigma}}{E^{N+1} - \varepsilon_F - E^N} + \frac{\Delta^2_{-,\Sigma}}{E^{N-1} + \varepsilon_F - E^N}. \tag{12}$$

H_K is a spin-flip scattering Hamiltonian in which the the two possible states of the scatterer flip their spins by means of $X_{\Uparrow,\Downarrow}$ and $X_{\Downarrow,\Uparrow}$ and, at the same time, they change their total angular momentum. Both the difference between $M_\Uparrow$ and $M_\Downarrow$, and the correlation effects included in the tunneling spectral amplitudes, are the reason why one must use spin-flip Hubbard operators instead of the usual spin-ladder operators $S^{(\pm)}$.

A crucial question is the sign of the exchange couplings (11) and (12). With our definitions (7), all the tunneling spectral amplitudes are positive. The sign of $\Delta_{+,\Uparrow}$ is the same than the one of $\Delta_{+,\Downarrow}$, and the same happens for $\Delta_{-,\Uparrow}$ with respect to $\Delta_{-,\Downarrow}$. Therefore, the signs of the exchange couplings are determined by the denominators. As, in the considered situation, the lowest energy corresponds to having N electrons in the QD, all the intermediate states $|I\rangle$, with $N \pm 1$ electrons in the QD and ∓ 1 electron at the Fermi level of the leads, have higher energy. Therefore, we have a very important result: *H_K has positive effective exchange couplings*. So, a Kondo Hamiltonian (10) with *antiferromagnetic couplings* (11) and (12) has been obtained. The conclusion is: *for any values of both N and S_z, the QD in the the presence of high B, presents Kondo physics.*

4. Exchange couplings and Kondo temperature (step 6)

The Hamiltonian (10) is equivalent to the standard Kondo Hamiltonian for $N = 1$. Any other measurable property deduced from Hamiltonian (10) as the temperature dependence of the conductance must present characteristics similar to the one found in the experiments involving just one electron [8, 9, 10, 11].

The important issue to be discussed in the general case of any N is the characteristic energy scale, T_K, which is determined by the antiferromagnetic couplings. J and J_Σ depend on both the energy difference $E^N - E^{N\pm1} \mp \varepsilon_F$, and tunneling spectral amplitudes $\Delta_{\pm,\Sigma}$. The former is practically independent on both N and Σ. Therefore, it does not imply any significant difference with respect to the well known case of $N = 1$. However interesting physical differences appear, through $\Delta_{\pm,\Sigma}$, depending on the weak or strong correlation nature of the states $|N, \Sigma\rangle$. Let us analyze the different situations as far as correlations are concerned:

i) Weak correlation

In order to simplify the discussion, let us consider the simple case of Fig. 1 where the weak correlation states are compact states

$$|N, \Uparrow\rangle = |C^K_{N-K}\rangle \ ; \ |N, \Downarrow\rangle = |C^{K+1}_{N-K-1}\rangle. \tag{13}$$

This is the simplest case in which

$$X_{\Uparrow,\Downarrow} = (-1)^K d^\dagger_{n=0,N-K-1,\uparrow} d_{n=0,K,\downarrow} \tag{14}$$

and similarly for the other Hubbard operators. We have also assumed, $|N-1\rangle = |C^K_{N-K-1}\rangle$ and $|N+1\rangle = |C^{K+1}_{N-K}\rangle$. In other case the quantum numbers of the $d^\dagger$ operators must be changed accordingly. Moreover, the signs are taken according with definitions (8). Due to the lack of correlation effects in the states, the tunneling spectral amplitudes are

$$\Delta_{-,\Uparrow} = \Delta_{+,\Downarrow} = V_{N-K-1}\,;\, \Delta_{-,\Downarrow} = \Delta_{+,\Uparrow} = V_K. \tag{15}$$

There is a difference between the antiferromagnetic couplings J, $J_\Uparrow$ and $J_\Downarrow$ due to the fact that $N-K-1 > K$. It is easier to tunnel from the leads to spin up states ($m = N-K-1$) within the QD because they are in the outer region of the QD while the first available spin down state ($m = K$) is in the inner region of the QD. This tunneling amplitude effect is not described by previous models of Kondo at finite B for $N = 1, 2$ [27, 28, 29], but has long been more broadly recognized both experimentally and theoretically for QD in the quantum Hall regime.

In this weak correlation regime the QD does not present any correlation effects, but the antiferromagnetic couplings are still a function of total energies and tunneling amplitudes. Since the Kondo temperature depends exponentially on J[26], it is a very sensitive magnitude with respect to many parameters as ω_0, B, V_i etc. However, this is not different from the case of just one electron in the QD in which experiments [8, 9, 10, 11] show T_K to be in the range of 1K. In any case, one can predict variations in T_K when the regime changes as discussed below.

ii) Strong correlation

In this case the discussion is much more complicated because for magnetic fields implying $\nu \geq 2$ we have not been able to find an analytical expression for the states. Therefore, we are going to make the discussion restricting us to the particular case of Fig. 1 in which the strongly correlated states skyrmion-like states of topological charge one [22, 23]. In this case, The Hubbard operators $X_{\Sigma,\Sigma'}$ have complicated, but analytical, expressions [19].

In some of the experiments showing chessboard conductance [17] N is of the order of 50. For such a large number of electrons, correlation effects provoke that $\Delta_{-,\Sigma}$ tends to zero. For instance, $\Delta_{-,\Sigma} \propto [NlnN]^{-1/2}$ for the skyrmion with the smallest size. This implies a quenching of the antiferromagnetic couplings due to the orthogonalization catastrophe. As a consequence, Kondo effect should not be observed when the number of electrons within the QD is large because the Kondo temperature is extremely small in this case.

In some other experiments showing chessboard conductance [16] N is lower than 10. In this case, correlation effects do not destroy Kondo effect but reduce $\Delta_{-,\Sigma}$ up to a factor of two [21]. The reduction of J and J_Σ

implies that Kondo temperatures are significantly smaller than for the case *i)* of compact states. In practice, one can move from the strong correlation regime *ii)* (lower part of Fig 1) to the weak correlation regime *i)* (upper part of Fig 1) by increasing an inplane component of the magnetic field. As a consequence of the above analysis, one should detect a clearly measurable increase of T_K during this process.

iii) There is a rather unusual case, for instance in the last step to the right in Fig. 2, in which the two lowest energy states with N electrons have spins differing in more than 1. Therefore, they can not be obtained from the same $|N-1\rangle$ by creating one electron with spin either up or down. In other words, one of the two states has a tunneling spectral amplitude equal to zero so that, for tunneling effects there is only a non degenerate GS and Kondo effect does not occur.

5. Chessboard behavior of the conductance (step 7)

A very characteristic feature of some experiments [16, 17, 18] is an alternating high-low conductance sequence as a function of B for a given temperature and number of electrons. When N is varied in ± 1, the high and low conductance regions are interchanged. Since a common way of representing the experimental results is to use a color-intensity scale for the conductance as a function of both B and a gate potential which varies N, the data present a chessboard aspect[16, 17, 18]. This occurs in a broad range of filling factors and number of electrons.

In the two level system approach[25] in which the two lowest states are separated by an energy splitting ΔE, Kondo-like behavior appears only when the experimental temperature is between $(\Delta E)^2/T_K$ and T_K (provided $\Delta E < T_K$) in order to have significant occupation of the two states. The quantitative application of the model would require the computation of both the energy splitting ΔE and Kondo temperature T_K which are very sensitive to many experimental parameters. Instead, a general understanding of the chessboard is obtained from the following qualitative explanation: as mention before, the main ingredient of our description is the alternation, when varying B, of weak and strong correlated GS of N within the QD. The second crucial point is that for weak correlation states, spectral amplitudes are much higher than for strong correlated states. These two features are depicted in the upper part of Fig. 3 where we have labelled the weak correlated states as compact states $|C_{1,2}\rangle$ while we have not given any name to the strongly correlated state. The important consequence of the alternation of high and low spectral functions is the alternation of high and low exchange couplings and consequently the same alternation of Kondo temperatures T_K which depends exponentially on the exchange coupling [26].

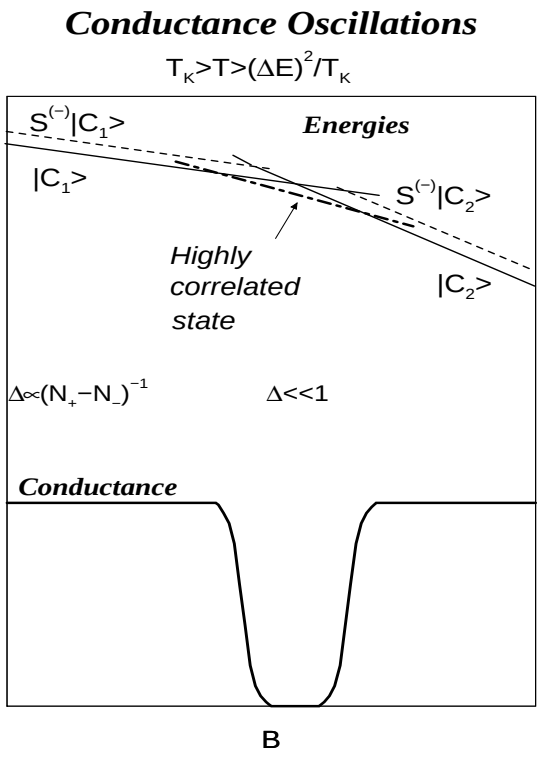

Figure 3. Schematic evolution with the magnetic field of the lowest energy states of N electrons within a QD (upper part). Continuous and dashed lines correspond to weak correlation states, while dashed-dotted lines correspond to strong correlation states. Kondo-like conductance (lower part) through such a QD in the range $T_K > T > \Delta E^2/T_K$ (see text).

Since the experiment is performed by fixing a temperature T, the strong oscillations of T_K imply that T alternates being lower (for weak correlation regions) and higher (for strong correlation regions) than T_K. In other words, $T < T_K$ for weak correlation regions, which means a high Kondo-like conductance. On the contrary, $T > T_K$ for strong correlation regions, which implies a quenching of the conductance. This is depicted in the lower part of Fig. 3. This explains the alternating behavior experimentally observed for fix gate voltage (i. e. number of electrons in the QD) and varying magnetic field.

The chessboard aspect also implies alternating low-high conductance regions for fix B and varying gate voltage. This is due to the fact that crossings for $N \pm 1$ electrons occur for magnetic fields roughly midway from crossings for N electrons[21] as depicted qualitatively in Fig. 4. By repeating the previous argument, one obtains the whole chessboard aspect

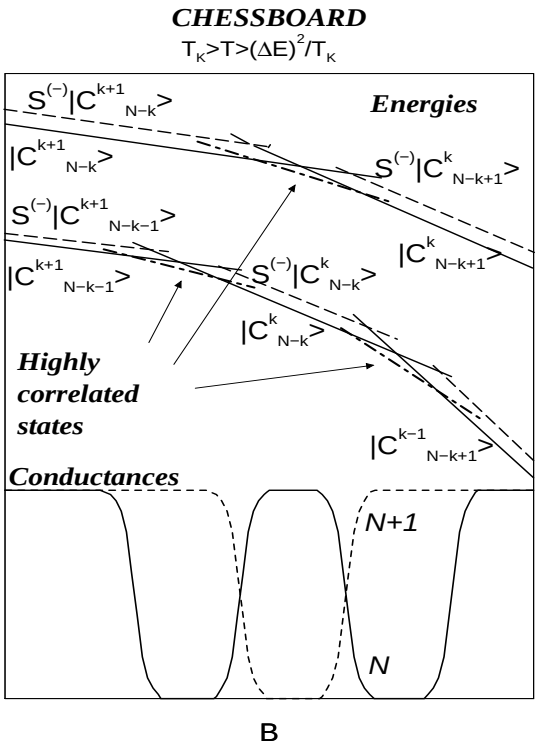

Figure 4. Schematic evolution with the magnetic field of the lowest energy states of N and $N+1$ electrons within a QD (upper part). Continuous and dashed lines correspond to weak correlation states, while dashed-dotted lines correspond to strong correlation states. Kondo-like conductance (lower part) through such a QD in the range $T_K > T > \Delta E^2/T_K$. The oscillations of the conductance are shifted between N and $N+1$ cases due to the dephasing between the positions of the crossing of GS in the two cases.

of the conductance schematically shown in lower part of Fig. 4.

Since Kondo-like behavior only occurs when the experimental temperature is in the range between $(\Delta E)^2/T_K$ and T_K, a clear prediction of our scheme is that the highly conducting regions of the chessboard would become narrower for decreasing temperature due to the lower limit condition.

6. Summary

We present a theoretical analysis of the chessboard aspect of the conductance through a QD in the Kondo regime. We perform a numerical calculation of the spectrum of N electrons in the isolated QD. Two alternating types of GS are found: strongly correlated and weakly correlated. By projecting onto the subspace of the two lowest eigenstates and coupling to the

leads, we get an effective Kondo Hamiltonian with antiferromagnetic exchange couplings depending on the QD properties. The main result of our description is the appearance of strong oscillations of the Kondo temperature due to strong oscillations of the spectral amplitude for strongly and weakly correlated states. This explains the chessboard oscillations of the experimental conductance measured at a fix temperature.

We make two predictions that can be experimentally checked:

1- The application of an inplane magnetic field provokes the transition from the regime of strong correlation to that of weak correlation. As a consequence, one should detect a clearly measurable increase of T_K during this process.

2- Since Kondo-like behavior only occurs when the experimental temperature is in the range $(\Delta E)^2/T_K < T < T_K$, the highly conducting regions of the chessboard would become narrower for decreasing temperature due to the lower limit condition.

Acknowledgements

We are grateful to J. Weis for useful discussions and providing us with experimental information. This work was supported in part by MEC (Spain) under contract No. PB96-0085, and CAM (Spain) under contract No. 07N/0064/2001.

References

1. L. I. Glazman and M. E. Raikh, Pis'ma Zh. Eksp. Teor. Fiz. **47**, 378 (1988) [JETP Lett. **47**, 452 (1988)].
2. T. K. Ng and P. A. Lee, Phys. Rev. Lett. **61**, 1768 (1988).
3. A. Kawabata, J. Phys. Soc. Jpn., **60**, 3222 (1991).
4. S. Hershfield, J. H. Davies, and J. W. Wilkins, Phys. Rev. Lett. **67**, 3720 (1991).
5. Y. Meir, N. S. Wingreen, and P. A. Lee, Phys. Rev. Lett. **70**, 2601 (1993).
6. A. Levy-Yeyati, A. Martin-Rodero and F. Flores, Phys. Rev. Lett., **71**, 2991 (1993).
7. K. A. Matveev, Phys. Rev. B, **51**, 1743 (1995).
8. D. Goldhaber-Gordon, J. Gores, M. A. Kastner, H. Shtrikman, D. Mahalu, U. Meirav, Nature **391**, 156 (1998); Phys. Rev. Lett. **81**, 5225 (1998).
9. S. M. Cronenwett, T. H. Oosterkamp, and L. P. Kouwenhoven, Science **281**, 540 (1998).
10. J. Schmid, J. Weis, K. Eberl, K. von Klitzing, Physica B, **256-258**, 182 (1998).
11. F. Simmel, R. H. Blick, J. P. Kotthaus, W. Wegscheider and M. Bichler, Phys. Rev. Lett. **83**, 804 (1999).
12. S. Sasaki, S. De Franceschi, J. M. Elzerman, W. G. van der Wiel, M. Eto, S. Tarucha, and L. P. Kouwenhoven, Nature, **405**, 764 (2000).
13. W. G. van der Wiel, S. De Franceschi, T. Fujisawa, J. M. Elzerman, S. Tarucha, and L. P. Kouwenhoven, Science, **289**, 2105 (2000).
14. Y. Ji, M. Heiblum, D. Sprinzak, D. Mahalu and H. Strikman, Science **290**, 779 (2000).
15. Y. Ji, M. Heiblum, and H. Strikman, Phys. Rev. Lett., **88**, 076601 (2002)
16. J. Schmid, J. Weis, K. Eberl, K. von Klitzing, Phys. Rev. Lett., **84**, 5824 (2000).

17. M. Keller, U. Wilhelm, J. Schmid, J. Weis, K. von Klitzing and K. Eberl, Phys. Rev. B., **64**, 033302 (2001).
18. D. Sprinzak, Y. Ji, M. Heiblum, D. Mahalu and H. Strikman, cond-mat/0109402.
19. C. Tejedor and L. Martin-Moreno, Phys. Rev. B, **63**, 035319 (2001).
20. P.G. Silvestrov and Y. Imry, cond-mat/0112308.
21. J.J. Palacios, L. Martin-Moreno, G. Chiappe and E. Louis and C. Tejedor, Phys. Rev. B, **50**, 5760 (1994) and references therein.
22. J. H. Oaknin, L. Martin-Moreno and C. Tejedor, Phys. Rev. B, **54**, 16850 (1996); erratum, **55**, 15943 (1997).
23. J. H. Oaknin, B. Paredes and C. Tejedor, Phys. Rev. B, **58**, 13028 (1998).
24. R. C. Ashoori, H. L. Stormer, J. S. Weiner, L. N. Pfeiffer, S. J. Pearton, K. W. Baldwin and K. W. West, Phys. Rev. Lett., **68**, 3088 (1992); *ibid* **71**, 613 (1993).
25. D. L. Cox and A. Zawadowski: *Exotic Kondo effects in Metals* (Taylor and Francis, London, 1999).
26. A. C. Hewson: *The Kondo problem to Heavy Fermions* (Cambridge University Press, Cambridge, 1993).
27. M. Pustilnik, Y. Avishai and K. Kikoin, Phys. Rev. Lett., **84**, 1756 (2000).
28. M. Eto and Y. V. Nazarov, Phys. Rev. Lett., **85**, 1306 (2000).
29. D. Giuliano and A. Tagliacozzo, Phys. Rev. Lett., **84**, 4677 (2000).